Improved Photocatalytic Activity and Characterization of Mixed TiO_2/SiO_2 and TiO_2/Al_2O_3 Materials

Carl Anderson and Allen J. Bard*

Department of Chemistry and Biochemistry, The University of Texas at Austin, Austin, Texas 78712

Received: August 30, 1996; In Final Form: November 23, 1996[⊗]

The characterization of mixed oxides of TiO_2/SiO_2 and TiO_2/Al_2O_3 prepared by sol−gel methods is described. Application of the TiO_2/Al_2O_3 material for the photocatalytic decomposition of salicylic acid gave improved activity relative to TiO_2-only materials. The photocatalytic activity of TiO_2/SiO_2, TiO_2/Al_2O_3, and TiO_2 toward the photocatalytic decomposition of phenol demonstrated the enhancement of local TiO_2 sites on TiO_2/SiO_2 materials relative to the other materials. The characterization of the catalysts indicates that the TiO_2/SiO_2 materials consist of matrix-isolated TiO_2 quantum particles, while the TiO_2/Al_2O_3 materials do not.

Introduction

Heinz Gerischer recognized very early the importance of semiconductor electrodes.[1] Following the introduction of TiO_2 single-crystal electrodes for solar energy conversion by Honda and Fujishima,[2] an enormous literature developed on the characterization and application of this material in photoelectrochemical applications. Photocatalysis at TiO_2 particles, with possible applications to waste treatment,[3,4] has been a particularly active area.[5,6] For such applications, it is important to improve the efficiency of the TiO_2-based photocatalysts. A strategy we have been investigating with such photocatalysts has been the combination of the photoactive TiO_2 material with an adsorbent. Not only does this provide preconcentration of the material near the photoactive sites, it also allows the possibility of adsorbing the material in the dark followed by later irradiation to decompose the material and restore the original photocatalyst. Studies of such materials also are of fundamental interest, because they allow one to probe such issues as the necessity of adsorption for decomposition in photocatalysis and whether photogenerated intermediates (like hydroxyl radical) escape the catalyst surface.[7] Moreover, this strategy allows the production of matrix-isolated quantum (Q-) particles of TiO_2 with a different band gap than the bulk material.

In an earlier study,[7] we demonstrated that a mixed oxide of TiO_2 and SiO_2 produced by a sol−gel method was a more efficient photocatalyst for the photocatalytic decomposition of rhodamine-6G (R-6G) than TiO_2 alone. The increase in efficiency was attributed to the presence of an adsorbent (SiO_2). The adsorbent phase increased the concentration of R-6G near the TiO_2 sites relative to the solution concentration. We also showed that while adsorption of R-6G was beneficial for photocatalytic activity of the catalysts, it was not a requirement. R-6G does not adsorb on TiO_2 alone, but the dissolved form is photodecomposed by a TiO_2 slurry.

The TiO_2/SiO_2 photocatalysts used in the earlier study[7] are characterized here. The enhanced photocatalytic activity of TiO_2 for the decomposition of salicylic acid in a mixed TiO_2/Al_2O_3 photocatalyst relative to pure TiO_2 is also demonstrated. The photocatalytic decomposition of phenol on TiO_2/SiO_2, TiO_2/Al_2O_3, and TiO_2 materials is also described. Further characterization of the TiO_2/SiO_2 materials was undertaken to understand better the increased efficiency of the materials. In particular, we want to explain the rapid rate of decomposition observed for R-6G adsorbed on the surface of the material. A better understanding of the size and phase of the TiO_2 domains in the materials aids in understanding their photocatalytic activity. Characteristics of the materials (TiO_2/SiO_2, TiO_2/Al_2O_3, and TiO_2), such as surface area, surface acidity, and their morphology (TiO_2/SiO_2 as a glass and TiO_2/Al_2O_3 as particles), were studied.

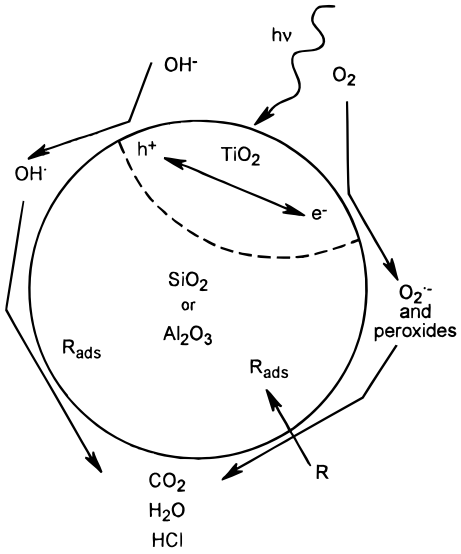

Figure 1. Schematic representation of the TiO_2/SiO_2 or TiO_2/Al_2O_3 photocatalyst with no interaction between the TiO_2 and SiO_2 or Al_2O_3 phases.

A schematic model for the mixed phase system is given in Figure 1. The TiO_2 and adsorbent (SiO_2 or Al_2O_3) are prepared so they are intimately mixed (on a 10 nm scale or smaller). The TiO_2 behaves as the photoactive center, e.g., generating hydroxyl radicals under irradiation, while the SiO_2 and Al_2O_3 provide better adsorption sites in the vicinity of the TiO_2. In actual particles there are many such domains on a single particle. Of interest is whether the particles behave as simple mixtures of the bulk materials, as mixtures of much smaller (quantum particle) domains, or as completely random intermixed phases.

The TiO_2/Al_2O_3 mixed catalysts were prepared by sol−gel methods to produce powders directly (as opposed to bulk glass materials for TiO_2/SiO_2 catalysts, which are ground in a ball mill). These materials were prepared by the uncatalyzed hydrolysis of the Ti and Al monomers. Preparation of particles

[⊗] Abstract published in *Advance ACS Abstracts,* March 1, 1997.

S1089-5647(96)02698-3 CCC: $14.00

obviates the need for mechanical grinding and offers a means of controlling particle size within the sol−gel synthesis to tailor the size of the particles for the desired application. We studied the adsorption and decomposition of aqueous salicylic acid (SA) on TiO_2/Al_2O_3 materials as a function of TiO_2 content and the photocatalytic decomposition of phenol on TiO_2/SiO_2, TiO_2/Al_2O_3, and TiO_2 materials. Both phenol and SA were stable to the reaction conditions when photocatalyst was not present. Phenol does not specifically adsorb to the materials used, but SA adsorbs to Al_2O_3. The TiO_2/SiO_2 materials were characterized by AFM and ^{29}Si CP-MAS NMR, and both TiO_2/SiO_2 and TiO_2/Al_2O_3 materials were examined by XRD and UV−vis reflection spectroscopy.

Experimental Section

Preparation of Photocatalysts. The preparation method for the TiO_2/SiO_2 materials has been described previously.[7] Sols of TiO_2/Al_2O_3 were prepared by the uncatalyzed hydrolysis of tetraisopropyl orthotitanate (TIOT, Fluka) and triisopropyl orthoaluminate (TIOA, 98%+, Aldrich). A solution of 20 g TIOA in 500 mL of 2-propanol (anhydrous, Baker) was prepared and stirred for 8 h. The solution was cooled to 0 °C and the quantity of TIOT necessary to give the desired Ti/Al ratio was added dropwise with stirring over the course of 1 h. While still at 0 °C, a molar quantity of water 4 times the total moles of TIOT and TIOA was added dropwise to the stirred solution. The resulting solution was slowly warmed to room temperature and stirred for 8 h. The mixture was allowed to age in the liquor for 7 days. After aging, the solvent was removed under vacuum at room temperature. The dry powder was stored for later heating and use. A material containing no TiO_2 was prepared by the same procedure except no TIOT was added, and the TIOA/2-propanol solution was not cooled to 0 °C before the addition of water. Materials of 90/10 and 95/5 (TiO_2/Al_2O_3 mole ratio) were prepared exactly as above, with the reaction scale reduced by a factor of 4.

The rates of photocatalytic decomposition of phenol (Aldrich) and salicylic acid (SA, Sigma) were determined directly with the molecule under study in an air-saturated aqueous solution. The conditions for the photocatalytic reactions were the same as previously reported:[7] 1 g/L of catalyst and initial concentrations of 3.7 mM phenol and 0.14 mM SA. The photoreactor was a Rayonet photochemical chamber reactor (RPR-100, Southern New England Ultraviolet Co., Harden, CT), the details of the reactor were given previously.[7]

Adsorption of SA on TiO_2/Al_2O_3 Materials. The adsorption of SA on TiO_2 and TiO_2/Al_2O_3 materials from the aqueous solutions was determined by a titration method. A 1 g/L slurry of the TiO_2/Al_2O_3 material with a volume of 135 mL was prepared and warmed to 40 °C, and this temperature was maintained throughout the experiment. SA was titrated into the solution; the concentration of SA in solution was 0.144 mM (measured by UV−vis absorbance, $A_{\lambda=308} = 0.600$). The slurry was stirred for 1 h to allow complete equilibration. The amount adsorbed was determined from the amount of SA added and the solution volume.

Characterization of Materials. An AFM image of a piece of 25/75 (TiO_2/SiO_2) glass was taken after the material was dried and before it was crushed. Images were recorded with a Nanoscope II with an AFM "J" head (Digital Instruments, Santa Barbara, CA) using a SiN tip. Surface area measurements were made using an Autosorb 1 gas sorption system (Quantachrome, NY). Resident software for BET analysis of Ar sorption isotherms at 77 K was used to determine surface area. Light scattering measurements were performed on a light table using a HeNe laser (638 nm) and a BI-2030 AT digital correlator (Brookhaven Instruments Corp., Holtsville, NY). The concentration of the sample started at ca. 0.1 g/L of catalyst in Millipore water filtered through Millipore Durapore 0.22 μM filters. The concentration was adjusted by addition of water until a satisfactory signal intensity was obtained. A solid state ^{29}Si MAS NMR spectrum of the 30/70 TiO_2/SiO_2 material heated to 200 °C was obtained using a cross-polarization (CP-MAS) pulse sequence. The spectrum was obtained with a Chemagnetics CMX-300 (Fort Collins, CO) operating at 60.0 MHz. The sample was spun at 3500 Hz. Powder X-ray diffraction measurements were made using a Philips Electronic Instruments X-ray diffractometer (Mount Vernon, NY) using a Cu (1.49 Å) anode. Samples were prepared by wet grinding catalysts with ethanol and casting a thin film from the slurry on a microscope slide of borosilicate glass by allowing the slurry to evaporate on the slide or by pressing the sample into a pellet (10 × 15 × 2.5 mm) in an aluminum frame. NaCl was used as the standard to determine instrumental peak broadening.

UV−vis reflectance measurements of powders were made using a RSA-MR-30 reflectance spectroscopy accessory (Labsphere Inc., North Sutton, NH) attached to a Milton Roy Spectronic 3000 diode array spectrophotometer (Milton Roy, San Leandro, CA). The samples were either bare (supported on filter paper) or placed in a sample holder with a quartz window. The thickness of the measured sample was such that no light passed through it. All spectra were obtained using an 8° sample positioning holder, giving total (diffuse and specular) reflectance relative to a calibrated standard SRS-010-99 (Labsphere Inc., North Sutton, NH). The reflectance data are reported as the $F(R_\infty)$ value from Kubelka−Munk theory vs the wavelength (or energy).[8] Band gap determinations were made by plotting $[F(R_\infty)h\nu]^2$ vs $h\nu$ (eV) and calculating the x intercept of a line for $0.1 < F(R_\infty) < 0.2$. Band gap measurements were made only for TiO_2, TiO_2/SiO_2, and TiO_2/Al_2O_3 materials that were not discolored. Further experimental details and results are available.[9]

Results and Discussion

Photodecomposition of Phenol. When an aqueous solution of phenol, which does not adsorb on either SiO_2 or Al_2O_3, was exposed to light in the presence of TiO_2/SiO_2, TiO_2/Al_2O_3, or TiO_2, the phenol concentration decreased exponentially with irradiation time. The rates are reported as pseudo-first-order rate constants for the purpose of comparing the relative efficiencies of the catalysts under identical reaction conditions. Figure 2 shows the measured rates of reaction as a function of the percentage of TiO_2 present in the material compared to the widely used Degussa TiO_2 powder. The concentration of phenol decreased negligibly over the time span of these experiments in the absence of a photocatalyst and in irradiated slurries of SiO_2 or Al_2O_3. The measured rate for the photocatalytic decomposition of phenol was slower for all of the mixed materials than for pure TiO_2. This is consistent with the idea of the photocatalyst consisting of two independent domains. When the SiO_2 or Al_2O_3 phase does not adsorb the molecule being decomposed (phenol), it decreases the activity of the catalyst by reducing the quantity of TiO_2 available for photoreactions relative to pure TiO_2. However, when the rates were normalized to the TiO_2 content of the material, the TiO_2/SiO_2 material demonstrated a more efficient use of the TiO_2 sites than TiO_2 alone or mixed TiO_2/Al_2O_3 materials. The normalized rate for the TiO_2/SiO_2 material was 6.7×10^{-3} min^{-1}; the rate for pure TiO_2 was 4.0×10^{-3} min^{-1}. The decreased reactivity of TiO_2 in TiO_2/Al_2O_3 materials was due to the decrease of

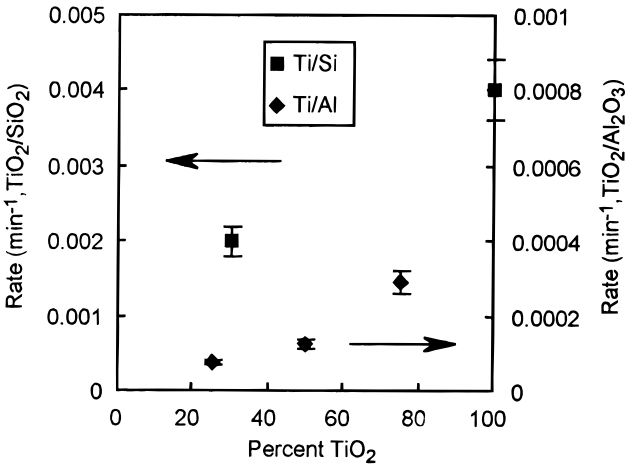

Figure 2. Rate constants for the photocatalytic decomposition of phenol on TiO_2/Al_2O_3, TiO_2/SiO_2 materials, pure TiO_2, and Degussa TiO_2 (square symbol at percent $TiO_2 = 100$). Initial phenol concentration = 3.7×10^{-9} M; catalyst concentration = 1 g/L.

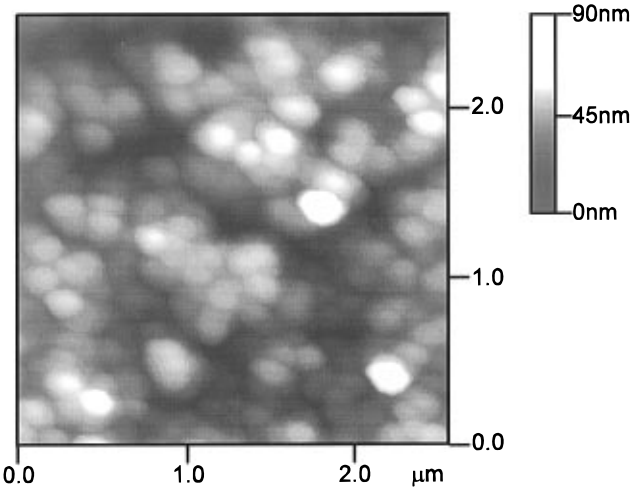

Figure 3. AFM image of 30/70 TiO_2/SiO_2 material (xerogel) prior to grinding.

available TiO_2 reactive sites on the catalysts without the benefit of adsorption to compensate for the lost activity. The normalized rate constants for 25/75, 50/50, and 75/25 TiO_2/Al_2O_3 materials were 3.0×10^{-4}, 2.5×10^{-4}, and 3.9×10^{-4} min^{-1}, respectively. The increase in the photocatalytic activity of the TiO_2 on TiO_2/SiO_2 materials is attributed to the presence of a mixed TiOSi phase at the TiO_2/SiO_2 interface. An interface of this type has been described for systems containing TiO_2 and SiO_2 and has been shown to possess sites of high Bronsted acidity.[10,11] Materials possessing regions of mixed TiOSi have been shown to increase the rate of oxidation of phenol by peroxide in heated aqueous solutions relative to one component TiO_2 or SiO_2 catalysts.[12] The increased activity in our materials is also attributed to this interface region. The TiOSi region served to activate the oxidation of phenol (via strong Bronsted acid sites). These regions should be in very close proximity to the TiO_2 sites. Oxidizing intermediates (such as $OH^{\bullet}$) are produced at the TiO_2 sites. The photocatalytic activity of the TiO_2/SiO_2 materials is enhanced by the chemical activation of phenol near the photoactive TiO_2 sites.

Characterization of TiO_2/SiO_2 Photocatalysts. The TiO_2/SiO_2 materials were characterized by AFM and ^{29}Si CP-MAS NMR. An AFM image of a 25/75 material is shown in Figure 3. Images of the 30/70 TiO_2/SiO_2 material had similar features. The image indicates that the material consists of ~200 nm spheres bonded together in a non-dense-packing arrangement.

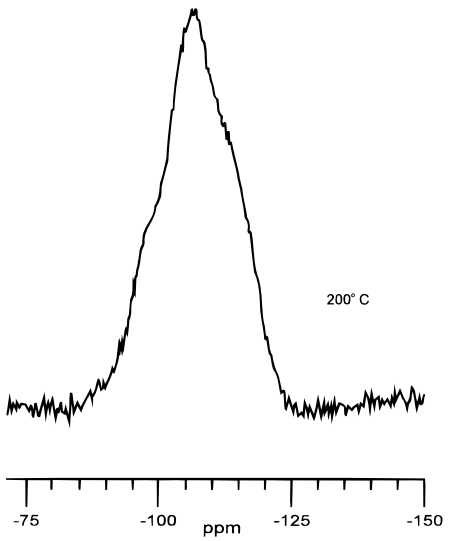

Figure 4. ^{29}Si CP-MAS NMR (60 MHz) spectra of a ground 30/70 TiO_2/SiO_2 material heated to 200 °C.

Note that these spheres are bonded together to form larger (5 μm) particles. The material, as it was used in photocatalytic reactions, consisted of ~5 μm particles (following mechanical grinding and sieving) made up of ~200 nm porous spheres bonded together. Thus, much of the reactive surface of the TiO_2/SiO_2 materials is located within the particles. This indicates that the reactivity of these materials might be improved if the materials were prepared as dispersed 200 nm spheres. By not allowing the spheres to bond together, material transport to the spheres in the interior of the porous particles would no longer be a potential hindrance to photocatalysis.

^{29}Si NMR studies of TiO_2/SiO_2 materials were undertaken to understand the environment around the Si atoms and understand the degree of mixing of Si and Ti in the catalysts. The chemical shift of the ^{29}Si signal is a function of the environment and can distinguish neighboring −OSi groups from neighboring −Ti groups.[13] Measurements were made with the 50/50, 75/25, and 30/70 materials and were compared to pure SiO_2. These measurements indicate that the average Si in the 30/70 material (Figure 4) had more −OTi groups around it than the other ratio materials. This is shown by the enhanced NMR signal in the Q_2 and Q_3 regions (equivalent to two and three −OTi groups around a Si, with shifts of $\delta \approx -90$ and −100 ppm, respectively)[13] for the 30/70 material relative to materials with different TiO_2/SiO_2 ratios. The presence of −OTi in the SiO_2 phase supports the idea of a mixed phase in these materials. The presence of a TiOSi phase is thought to be responsible for the enhanced adsorption of R-6G on 30/70 materials relative to those with higher SiO_2 ratios.[7] The 30/70 material represented the optimum ratio for achieving the largest TiOSi interface area. As the fraction of TiO_2 decreased, the Ti was incorporated into the SiO_2 matrix,[11] leaving little bulk TiO_2 to form a TiOSi interface. At higher TiO_2 ratios, the TiO_2 and SiO_2 phases tended to segregate again, producing mixed phases and a diminished interface region. TiO_2/SiO_2 materials with ratios close to 30/70 exhibit indications of a significant Ti−O−Si phase.[10,11]

Effect of TiO_2/Al_2O_3 Ratio on Photocatalytic Decomposition of SA. The measured rate constants for the photocatalytic decomposition of SA (which adsorbs on Al_2O_3) are shown in Figure 5 as a function of TiO_2 percentage. The region of % TiO_2 = 75−90% gave the greatest activity, about twice the activity of Degussa TiO_2. This increase in activity can be partially attributed to the increased surface area of the mixed

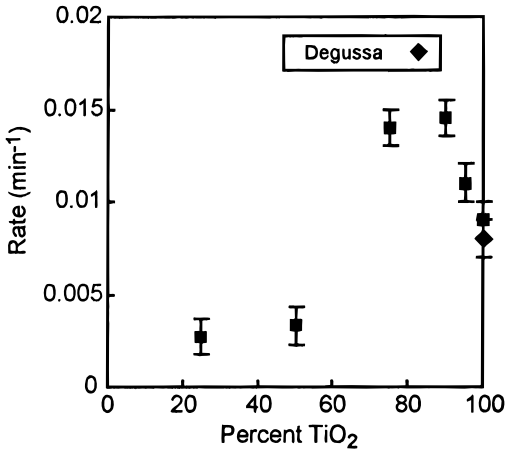

Figure 5. Rate constants for the photocatalytic decomposition of salicylic acid on TiO_2/Al_2O_3 materials and pure TiO_2. Initial SA concentration = 1.4×10^{-4} M; catalyst concentration = 1 g/L.

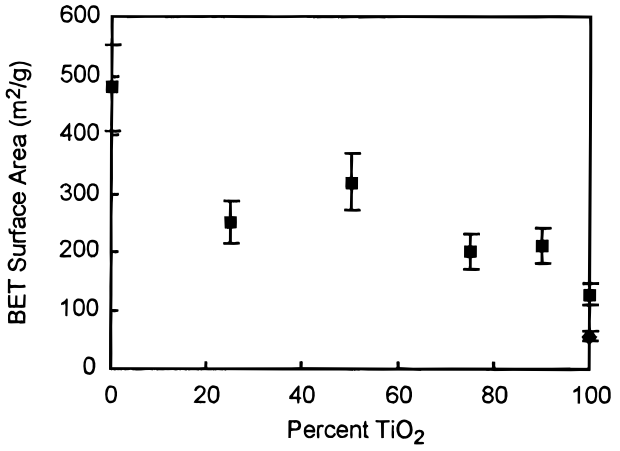

Figure 6. BET surface areas from Ar sorption isotherms at 77 K for TiO_2/Al_2O_3 materials as a function of the percentage of TiO_2 in the material.

materials (Figure 6). However, if these results were normalized for TiO_2 content of the material, we observed that the TiO_2/Al_2O_3 materials used the TiO_2 sites more effectively than did Degussa. This is thought to be the result of adsorption of SA on the Al_2O_3 near the TiO_2 sites, thereby increasing the concentration of SA at the surface relative to the solution concentration in a manner analogous to that previously discussed for R-6G on TiO_2/SiO_2.[7] The increased activity for the 75/25 TiO_2/Al_2O_3 material is due to the favorable balance between enhanced reactivity of individual TiO_2 sites by adsorption of SA near those sites and the loss of catalyst activity by the replacement of the active TiO_2 sites with nonphotoactive Al_2O_3.

Adsorption of SA on TiO_2/Al_2O_3. The adsorption of SA on TiO_2/Al_2O_3 materials from a 0.144 mM SA solution indicates that the adsorption is a function of the Al_2O_3 content in the materials (Figure 7). The concentration used for the quantification of adsorption of SA on TiO_2/Al_2O_3 materials was 0.144 mM, the starting concentration of the SA in photocatalytic reactions. The quantity of SA added (less the amount remaining in solution) was normalized to the surface area of catalyst present, and the results were reported as Γ_{SA} (mol/m^2). Unlike the adsorption of R-6G on TiO_2/SiO_2 experiments,[7] this result indicates that the properties of the final material are simply a mixture of the individual properties of TiO_2 and Al_2O_3, because the adsorption is essentially proportional to the Al_2O_3 content of the material.

Characterization of TiO_2/Al_2O_3. The BET surface areas of the TiO_2/Al_2O_3 materials are shown as a function of TiO_2 content in Figure 6. The surface area of the material roughly correlates with the Al_2O_3 content in the material. This further supports the idea that the final TiO_2/Al_2O_3 materials are a mixture (with very little chemical interaction) of the TiO_2 and Al_2O_3 properties. Since the TiO_2 materials formed by these processes have lower surface areas than the Al_2O_3 materials, the surface area increases result from the Al_2O_3.

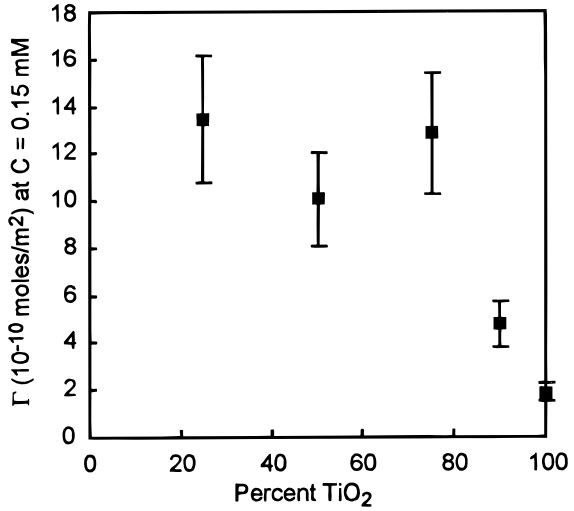

Figure 7. Single-point adsorption measurements for the adsorption of SA on TiO_2/Al_2O_3 materials as a function of the percentage of TiO_2 in the material. Final SA concentration = 1.4×10^{-4} M; catalyst concentration = 1 g/L.

Dynamic light scattering measurements were performed on the TiO_2/Al_2O_3 powders to determine average particle sizes for the materials. These measurements indicated that particle size was not a function of the TiO_2/Al_2O_3 ratio and all had similar sizes of $1.3 \pm 0.5\ \mu$m. This indicates that the Al_2O_3 controlled the final particle size, because the ratio of 2-propanol to TIOA was constant through all the reactions. Because both the TiO_2/SiO_2 and TiO_2/Al_2O_3 materials can be made as either bulk glassy solids (as the TiO_2/SiO_2 materials were) or powders (as the TiO_2/Al_2O_3 materials were), the sol−gel process conditions control the form of the final catalyst material.

Analysis of TiO_2 in TiO_2/SiO_2 and TiO_2/Al_2O_3 Materials. The physical form of TiO_2 in the mixed materials is important to the photocatalytic activity of the materials. And the size of the TiO_2 domains affects the distance between the TiO_2 centers and thus the distance an oxidizing intermediate ($OH^{\bullet}$) would have to travel before reacting with an adsorbed species on the SiO_2 or Al_2O_3 phase. An ideal material would be one in which the particles were large enough to give bulk anatase behavior (e.g., no quantum effects that increase the band gap) and still achieve maximum mixing of the TiO_2 and SiO_2 or Al_2O_3.

XRD of TiO_2/SiO_2 and TiO_2/Al_2O_3 Materials. XRD patterns of the materials studied gave the expected patterns for TiO_2 anatase or rutile phases when measured crystalline domains were greater than 5 nm. Powder XRD results are summarized in Figure 8. When the TiO_2/Al_2O_3 materials were heated to 1000 °C, the thermodynamically favored rutile phase of TiO_2 was formed. The TiO_2 domains were larger than 100 nm for the 75/25 TiO_2/Al_2O_3 and the pure TiO_2 samples heated to 1000 °C. The growth of organized TiO_2 domains and the phase (anatase or rutile) of those domains was controlled by the fraction of TiO_2 in the material and the temperature to which it was heated. For pure TiO_2 samples, an anatase TiO_2 phase was present at the outset and grew with increasing temperature. At 625 °C the rutile phase began to form, and the anatase was completely transformed to rutile by 1000 °C. As the fraction of TiO_2 was decreased in the TiO_2/Al_2O_3 material, the temper-

	30/70 (Ti/Si)	25/75 (Ti/Al)	50/50 (Ti/Al)	75/25 (Ti/Al)	100/0 (TiO_2)
1000° C	A-11	R-48	R-43	R>100	R>100
750° C	A-5	R-13 A-14	R-15 A-16	R-35 A-18	R-67 A-62
625° C	N	N	A-13	A-13	R-26 A-32
500° C	N	N	N	A-13	A-30
200° C	N	N	N	N	A-11

Figure 8. Crystalline phases determined by powder XRD for materials heated to different temperatures for 12 h. The crystallite sizes were determined using the Scherrer equation for line width broadening. N, no crystalline phase was detected; A, anatase phase only (size of crystallites in nm); R, rutile phase only (size of crystallites in nm).

ature necessary for the crystallization of anatase, and the subsequent initial transformation to rutile increased. This is due to the increased separation of the TiO_2 domains as the fraction of TiO_2 decreases. At lower TiO_2 ratios, the initial TiO_2 domains are smaller, and hence greater heat is required to drive the crystallization.

The interaction between TiO_2 and SiO_2 in the 30/70 TiO_2/SiO_2 material was demonstrated in the crystallization behavior of TiO_2 in that material (see Figure 8). The TiO_2 never formed a rutile phase as it did in the TiO_2/Al_2O_3 materials. This is due to the stabilization of the anatase phase by the surrounding SiO_2 phase through the TiOSi interface. At the interface, TiO_2 atoms are substituted into the tetrahedral SiO_2 lattice forming tetrahedral Ti sites. The interaction between the tetrahedral Ti species and the octahedral Ti sites in the anatase is thought to prevent the transformation to rutile.[14] The SiO_2 lattice locks the Ti−O species at the interface with the TiO_2 domains preventing the nucleation that is necessary for the phase transformation to rutile.

UV−Vis Reflectance of TiO_2/SiO_2 and TiO_2/Al_2O_3 Materials. The TiO_2 in the materials were studied by UV−vis reflectance, and a plot of the square of the absorbed light [proportional to the square of the Kubelka−Munk function $F(R_\infty)$] vs the energy of irradiation was used to obtain the band gap E_g. This optical absorption behavior is consistent with a direct band gap semiconductor. The Kubelka−Munk function is given by

$$F(R_\infty) = (1 - R_\infty)^2/2R_\infty = K/S \qquad (1)$$

where R_∞ is the measured reflectance ($R_\infty = R_{sample}/R_{standard}$), K is the absorption coefficient, and S is the scattering coefficient.[8] The use of $F(R_\infty)$ as the equivalent of absorbance relies on the assumption that the scattering coefficients were consistent throughout the compared samples. This assumption was validated by the comparison of the reflectance spectra of the materials studied (TiO_2/SiO_2 and TiO_2/Al_2O_3) at wavelengths longer than the TiO_2 absorption (450−900 nm). The $F(R_\infty)$ value in nonadsorbing regions was a function of S only, thus allowing the verification of the similarity of S values.

TiO_2 domain sizes too small to estimate by XRD (∼1 nm) were obtained from the blue shift in the absorption onset. The shift in E_g can be used to find the approximate organized domain size from the relationship derived by Brus[15] from a particle in a sphere model for relating band gap shift (ΔE_g) to particle radius

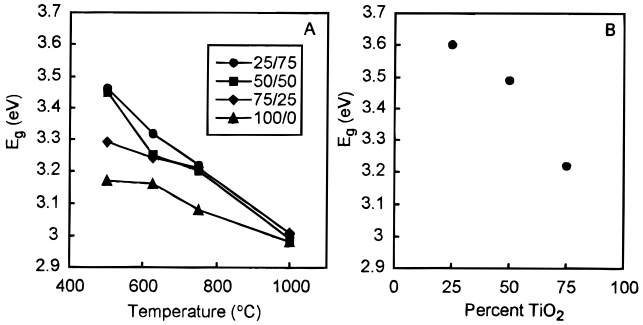

Figure 9. Band gap (E_g) of (A) TiO_2/Si_2 and (B) TiO_2/Al_2O_3 materials measured by UV−vis reflectance as a function of (A) temperature and (B) percentage of TiO_2 in the material (at 200 °C).

$$\Delta E_g = \left(\frac{\hbar^2\pi^2}{2r^2}\frac{1}{\mu}\right) - \frac{1.8e^2}{r\epsilon} \qquad (2)$$

where r is the radius of the particle, ϵ is the dielectric constant of the materials, and μ is the reduced mass of the excition calculated from

$$\mu^{-1} = m_e^* + m_h^* \qquad (3)$$

where m_e^* is the mass of the electron and m_h^* is the mass of the hole. ϵ has been measured as 184,[15] and μ has been calculated as $1.63m_e$ (mass of electron at rest).[16] For a 50/50 TiO_2/Al_2O_3 material heated to 500 °C, a $\Delta E_g = 0.25$ eV was measured, yielding from eq 2 a particle radius of 9 Å. This estimated size is subject to substantial error because of the assumptions that μ and ϵ for the bulk TiO_2 are valid for the nanocrystalline TiO_2.[15−17]

Knowledge of E_g is also important in determining the energy of the light absorbed to generate electron−hole pairs. When the TiO_2 domains are sufficiently large (>3 nm), the E_g will be at or very near the bulk value (3.0 eV for rutile and 3.2 eV for anatase). An increase of E_g for the TiO_2 shows the existence of quantum effects and smaller organized TiO_2 domains. The trend observed here was that the lower the percentage of TiO_2, the smaller the TiO_2 particle size (larger E_g). Figure 9A shows the growth of the TiO_2 domains in TiO_2/SiO_2 materials as a function of temperature of photocatalyst preparation. For the TiO_2/SiO_2 materials prepared at 500−600 °C, the TiO_2 domains are very small (less than 3 nm), and the catalyst consists of matrix-isolated Q-particles. At higher temperatures, the domains grow to anatase material and finally to rutile at 1000 °C. However, the anatase to rutile conversion rate depends on composition, so that the 25/75 material remained in the anatase phase, even at 1000 °C. The behavior of the TiO_2/Al_2O_3 was different. For ratios below 50/50, the TiO_2 particle size was smaller (as indicated by the larger E_g; Figure 9B); however, the bulk phases grew more rapidly with temperature compared to TiO_2/SiO_2 (Figure 8). The results suggest that the TiOSi interface stabilizes the TiO_2 domains, hindering the agglomeration of TiO_2 and thus preventing their growth. The 30/70 material displayed quantum effects after being heated to 500 °C; when the material was heated to only 200 °C, the TiO_2 domains were probably smaller and consequently were also isolated Q-particles. The ideal TiO_2/SiO_2 photocatalyst design would maximize the adsorption behavior and the proximity of the SiO_2 adsorption zones to TiO_2 photoactive ones (which

would favor smaller domains) and minimize E_g. The advantages of the TiOSi phase outweigh the potential loss of activity due to the loss of absorption of lower energy light due to quantum effects. The TiO_2/Al_2O_3 materials demonstrated better activity when heated to a temperature sufficient to give bulk TiO_2 (anatase) behavior.

Conclusions

Improved photocatalysts can be prepared by fabricating composite materials through sol−gel processing. These materials combine the photocatalytic properties of TiO_2 and the adsorptive properties of SiO_2 or Al_2O_3. In the TiO_2/SiO_2 material the TiO_2 showed quantum particle effects characteristic of very small domains and a large amount of TiOSi structure. The more acidic SiO_2 sites promote the adsorption of rhodamine 6G and a higher decomposition rate than on pure TiO_2. The TiO_2/Al_2O_3 materials behave more as a composite of the two bulk phases. The basic Al_2O_3 adsorbed acidic species and showed improved photocatalytic decomposition of salicylic acid.

Acknowledgment. The support of this work by the National Science Foundation (CHE9423874) and the National Renewable Energy Laboratory is gratefully acknowledged. We thank Professor Phil Bennet for the BET analyses.

References and Notes

(1) (a) Gerischer, H. *Z. Phys. Chem. (Munich)* **1961**, *27*, 48. (b) Gerischer, H. In *Advances in Electrochemistry and Electrochemical Engineering*; Delahay, P., Ed.; Interscience: New York, 1961; Vol. 1, p 139.
(2) Fujishima, A.; Honda, K. *Nature (London)* **1972**, *238*, 37.
(3) Frank, S. N.; Bard, A. J. *J. Am. Chem. Soc.* **1977**, *99*, 303.
(4) Bard, A. J. *J. Photochem.* **1979**, *10*, 59.
(5) *Photocatalytic Purification and Treatment of Water and Air*; Ollis, D. F., Al-Ekabi, H., Eds.; Elsevier: Amsterdam, 1993.
(6) Schwitzgebel, J.; Ekerdt, J. G.; Gerischer, H.; Heller, A. *J. Phys. Chem.* **1995**, *99*, 5633.
(7) Anderson, C.; Bard, A. J. *J. Phys. Chem.* **1995**, *99*, 9882.
(8) Kortum, G. *Reflectance Spectroscopy*; Springer-Verlag: New York, 1969.
(9) Anderson, C. Ph.D. Dissertation, University of Texas at Austin, Dec 1995.
(10) Lassaletta, G.; Fernandez, A.; Espinos, J. P.; Gonzalez-Elipe, A. R. *J. Phys. Chem.* **1995**, *99*, 1484.
(11) Galan-Fereres, M.; Alemany, L. J.; Mariscal, R.; Banares, M. A.; Anderson, J. A.; Pierre, J. L. G. *Chem. Mater.* **1995**, *7*, 1342.
(12) Kooyman, P. J.; van der Wall, P.; Verdaasdonk, P. A. J.; Jansen, K. C.; van Bekkum, H. *Catal. Lett.* **1992**, *13*, 229.
(13) Colin, A. F. *Solid State NMR for Chemists*; CRC Press: Ontario, 1983.
(14) Brinker, C. J.; Scherer, G. W. *Sol-Gel Science*; Academic Press: Boston, 1990.
(15) Brus, L. E. *J. Chem. Phys.* **1983**, *79*, 5566.
(16) Kormann, C.; Bahnemann, D. W.; Hoffmann, M. R. *J. Phys. Chem.* **1988**, *92*, 5196.
(17) Pankove, J. *Optical Processes in Semiconductors*; Dover Publications: New York, 1971.